Chapter 3

Elementary Applications of the Basic Equations

In addition to the geostrophic wind, which was discussed in Chapter 2, there are other approximate expressions for the relationships among velocity, pressure, and temperature fields that are useful in the analysis of weather systems. We consider estimates of the wind that derive from fundamental force balances, trajectory and streamline analysis, the thermal wind, and estimates for vertical motion and surface pressure tendency.

3.1 BASIC EQUATIONS IN ISOBARIC COORDINATES

The topics are discussed most conveniently using a coordinate system in which pressure is the vertical coordinate. Thus, before introducing the elementary applications of the present chapter, it is useful to present the dynamical equations in isobaric coordinates.

3.1.1 The Horizontal Momentum Equation

The approximate horizontal momentum equations (2.24) and (2.25) may be written in vectorial form as

$$\frac{D\mathbf{V}}{Dt} + f\,\mathbf{k} \times \mathbf{V} = -\frac{1}{\rho}\nabla p \qquad (3.1)$$

where $\mathbf{V} = \mathbf{i}u + \mathbf{j}v$ is the *horizontal* velocity vector. In order to express (3.1) in isobaric coordinate form, we transform the pressure gradient force using (1.33) and (1.34) to obtain

$$\frac{D\mathbf{V}}{Dt} + f\,\mathbf{k} \times \mathbf{V} = -\boldsymbol{\nabla}_p \Phi \qquad (3.2)$$

where $\boldsymbol{\nabla}_p$ is the horizontal gradient operator applied with pressure held constant.

An Introduction to Dynamic Meteorology. DOI: 10.1016/B978-0-12-384866-6.00003-9

Because p is the independent vertical coordinate, we must expand the total derivative as

$$\begin{aligned}\frac{D}{Dt} &\equiv \frac{\partial}{\partial t} + \frac{Dx}{Dt}\frac{\partial}{\partial x} + \frac{Dy}{Dt}\frac{\partial}{\partial y} + \frac{Dp}{Dt}\frac{\partial}{\partial p} \\ &= \frac{\partial}{\partial t} + u\frac{\partial}{\partial x} + v\frac{\partial}{\partial y} + \omega\frac{\partial}{\partial p}\end{aligned} \tag{3.3}$$

Here $\omega \equiv Dp/Dt$ (usually called the "omega" vertical motion) is the pressure change following the motion, which plays the same role in the isobaric coordinate system that $w \equiv Dz/Dt$ plays in height coordinates. We note that the partial derivatives with respect to x and y are taken with pressure held constant—that is, on isobaric surfaces.

From (3.2) we see that the isobaric coordinate form of the geostrophic relationship is

$$f\mathbf{V}_g = \mathbf{k} \times \nabla_p \Phi \tag{3.4}$$

One advantage of isobaric coordinates is easily seen by comparing (2.23) and (3.4). In the latter equation, density does not appear. Thus, a given geopotential gradient implies the same geostrophic wind at any height, whereas a given horizontal pressure gradient implies different values of the geostrophic wind depending on the density. Furthermore, if f is regarded as a constant, the horizontal divergence of the geostrophic wind at constant pressure is zero:

$$\nabla_p \cdot \mathbf{V}_g = 0$$

3.1.2 The Continuity Equation

It is possible to transform the continuity equation (2.31) from height coordinates to pressure coordinates. However, it is simpler to directly derive the isobaric form by considering a Lagrangian control volume $\delta V = \delta x \delta y \delta z$ and applying the hydrostatic equation $\delta p = -\rho g \delta z$ (note that $\delta p < 0$) to express the volume element as $\delta V = -\delta x \delta y \delta p/(\rho g)$. The mass of this fluid element, which is conserved following the motion, is then $\delta M = \rho \delta V = -\delta x \delta y \delta p/g$. Thus,

$$\frac{1}{\delta M}\frac{D}{Dt}(\delta M) = \frac{g}{\delta x \delta y \delta p}\frac{D}{Dt}\left(\frac{\delta x \delta y \delta p}{g}\right) = 0$$

After differentiating, using the chain rule, and changing the order of the differential operators, we obtain[1]

$$\frac{1}{\delta x}\delta\left(\frac{Dx}{Dt}\right) + \frac{1}{\delta y}\delta\left(\frac{Dy}{Dt}\right) + \frac{1}{\delta p}\delta\left(\frac{Dp}{Dt}\right) = 0$$

[1] From now on g will be regarded as a constant.

or

$$\frac{\delta u}{\delta x} + \frac{\delta v}{\delta y} + \frac{\delta \omega}{\delta p} = 0$$

Taking the limit δx, δy, $\delta p \to 0$ and observing that δx and δy are evaluated at constant pressure, we obtain the continuity equation in the isobaric system:

$$\left(\frac{\partial u}{\partial x} + \frac{\partial v}{\partial y}\right)_p + \frac{\partial \omega}{\partial p} = 0 \tag{3.5}$$

This form of the continuity equation contains no reference to the density field and does not involve time derivatives. The simplicity of (3.5) is one of the chief advantages of the isobaric coordinate system.

3.1.3 The Thermodynamic Energy Equation

The first law of thermodynamics (2.43) can be expressed in the isobaric system by letting $Dp/Dt = \omega$ and expanding DT/Dt using (3.3):

$$c_p\left(\frac{\partial T}{\partial t} + u\frac{\partial T}{\partial x} + v\frac{\partial T}{\partial y} + \omega\frac{\partial T}{\partial p}\right) - \alpha\omega = J$$

This may be rewritten as

$$\left(\frac{\partial T}{\partial t} + u\frac{\partial T}{\partial x} + v\frac{\partial T}{\partial y}\right) - S_p\omega = \frac{J}{c_p} \tag{3.6}$$

where, with the aid of the equation of state and Poisson's equation (2.44), we have

$$S_p \equiv \frac{RT}{c_p p} - \frac{\partial T}{\partial p} = -\frac{T}{\theta}\frac{\partial \theta}{\partial p} \tag{3.7}$$

which is the static stability parameter for the isobaric system. Using (2.49) and the hydrostatic equation, (3.7) may be rewritten as

$$S_p = (\Gamma_d - \Gamma)/\rho g$$

Thus, S_p is positive provided that the lapse rate is less than dry adiabatic. However, because density decreases approximately exponentially with height, S_p increases rapidly with height. This strong height dependence of the stability measure S_p is a minor disadvantage of isobaric coordinates.

3.2 BALANCED FLOW

Despite the apparent complexity of atmospheric motion systems as depicted on synoptic weather charts, the pressure (or geopotential height) and velocity distributions in meteorological disturbances are actually related by rather simple approximate force balances. In order to gain a qualitative understanding of the horizontal balance of forces in atmospheric motions, we idealize by considering flows that are steady state (i.e., time independent) and have no vertical component of velocity. Furthermore, it is useful to describe the flow field by expanding the isobaric form of the horizontal momentum equation (3.2) into its components in a so-called *natural* coordinate system.

3.2.1 Natural Coordinates

The natural coordinate system is defined by the orthogonal set of unit vectors **t**, **n**, and **k**. Unit vector **t** is oriented parallel to the horizontal velocity at each point; unit vector **n** is normal to the horizontal velocity and is oriented so that it is positive to the left of the flow direction; and unit vector **k** is directed vertically upward. In this system the horizontal velocity may be written $\mathbf{V} = V\mathbf{t}$, where V, the horizontal speed, is a nonnegative scalar defined by $V \equiv Ds/Dt$, where $s(x, y, t)$ is the distance along the curve followed by a parcel moving in the horizontal plane. The acceleration following the motion is thus

$$\frac{D\mathbf{V}}{Dt} = \frac{D(V\mathbf{t})}{Dt} = \mathbf{t}\frac{DV}{Dt} + V\frac{D\mathbf{t}}{Dt}$$

The rate of change of **t** following the motion may be derived from geometrical considerations with the aid of Figure 3.1:

$$\delta\psi = \frac{\delta s}{|R|} = \frac{|\delta\mathbf{t}|}{|\mathbf{t}|} = |\delta\mathbf{t}|$$

Here R is the *radius of curvature* following the parcel motion, and we have used the fact that $|\mathbf{t}| = 1$. By convention, R is taken to be positive when the center of curvature is in the positive **n** direction. Thus, for $R > 0$, the air parcels turn

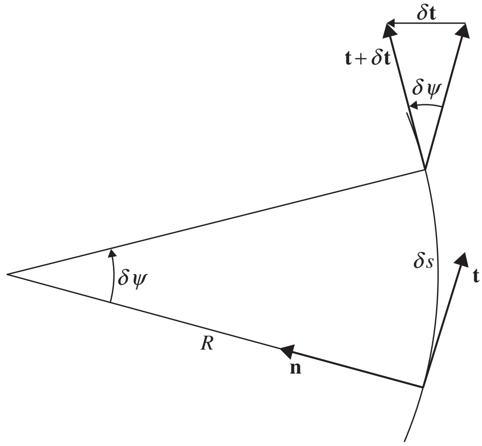

FIGURE 3.1 Rate of change of the unit tangent vector **t** following the motion.

toward the left following the motion, and for $R < 0$, the air parcels turn toward the right following the motion.

Noting that in the limit $\delta s \to 0$, $\delta\mathbf{t}$ is directed parallel to $\mathbf{n}$, the preceding relationship yields $D\mathbf{t}/Ds = \mathbf{n}/R$. Thus,

$$\frac{D\mathbf{t}}{Dt} = \frac{D\mathbf{t}}{Ds}\frac{Ds}{Dt} = \frac{\mathbf{n}}{R}V$$

and

$$\frac{D\mathbf{V}}{Dt} = \mathbf{t}\frac{DV}{Dt} + \mathbf{n}\frac{V^2}{R} \tag{3.8}$$

Therefore, the acceleration following the motion is the sum of the rate of change of speed of the air parcel and its centripetal acceleration due to the curvature of the trajectory. Because the Coriolis force always acts normal to the direction of motion, its natural coordinate form is simply

$$-f\,\mathbf{k} \times \mathbf{V} = -f\,V\mathbf{n}$$

whereas the pressure gradient force can be expressed as

$$-\nabla_p\Phi = -\left(\mathbf{t}\frac{\partial\Phi}{\partial s} + \mathbf{n}\frac{\partial\Phi}{\partial n}\right)$$

The horizontal momentum equation may thus be expanded into the following component equations in the natural coordinate system:

$$\frac{DV}{Dt} = -\frac{\partial\Phi}{\partial s} \tag{3.9}$$

$$\frac{V^2}{R} + f\,V = -\frac{\partial\Phi}{\partial n} \tag{3.10}$$

Equations (3.9) and (3.10) express the force balances parallel to and normal to the direction of flow, respectively. For motion parallel to the geopotential height contours, $\partial\Phi/\partial s = 0$, and the speed is constant following the motion. If, in addition, the geopotential gradient normal to the direction of motion is constant along a trajectory, (3.10) implies that the radius of curvature of the trajectory is also constant. In that case the flow can be classified into several simple categories depending on the relative contributions of the three terms in (3.10) to the net force balance.

3.2.2 Geostrophic Flow

Flow in a straight line ($R \to \pm\infty$) parallel to height contours is referred to as *geostrophic motion*. In geostrophic motion the horizontal components of the Coriolis force and pressure gradient force are in exact balance so that $V = V_g$,

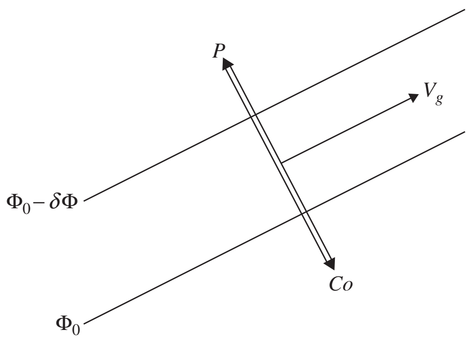

FIGURE 3.2 Balance of forces for geostrophic equilibrium. The pressure gradient force is designated by P and the Coriolis force by Co.

where the geostrophic wind V_g is defined by[2]

$$f V_g = -\partial\Phi/\partial n \tag{3.11}$$

This balance is indicated schematically in Figure 3.2. The actual wind can be in exact geostrophic motion only if the height contours are parallel to latitude circles. As discussed in Section 2.4.1, the geostrophic wind is generally a good approximation to the actual wind in extratropical synoptic-scale disturbances. However, in some of the special cases treated later, this is not true.

3.2.3 Inertial Flow

If the geopotential field is uniform on an isobaric surface so that the horizontal pressure gradient vanishes, (3.10) reduces to a balance between Coriolis force and centrifugal force:

$$V^2/R + f V = 0 \tag{3.12}$$

Equation (3.12) may be solved for the radius of curvature

$$R = -V/f$$

Since from (3.9), the speed must be constant in this case, the radius of curvature is also constant (neglecting the latitudinal dependence of f). Thus, the air parcels follow circular paths in an anticyclonic sense.[3] The period of this

[2]Note that although the actual speed V must always be positive in the natural coordinates, V_g, which is proportional to the height gradient normal to the direction of flow, may be negative, as in the "anomalous" low shown later in Figure 3.5c.

[3]Anticyclonic flow is a clockwise rotation in the Northern Hemisphere and counterclockwise in the Southern Hemisphere. Cyclonic flow has the opposite sense of rotation in each hemisphere.

oscillation is

$$P = \left|\frac{2\pi R}{V}\right| = \frac{2\pi}{|f|} = \frac{\frac{1}{2}\text{ day}}{|\sin\phi|} \tag{3.13}$$

P is equivalent to the time that is required for a Foucault pendulum to turn through an angle of 180°. Thus, it is often referred to as one-half *pendulum day*.

Because both the Coriolis force and the centrifugal force due to the relative motion are caused by inertia of the fluid, this type of motion is traditionally referred to as an *inertial oscillation*, and the circle of radius $|R|$ is called the inertia circle. It is important to realize that the "inertial flow" governed by (3.12) is not the same as inertial motion in an absolute reference frame. The flow governed by (3.12) is just the constant angular momentum oscillation referred to in Section 1.3.4. In this flow the force of gravity, acting orthogonal to the plane of motion, keeps the oscillation on a horizontal surface. In true inertial motion, all forces vanish and the motion maintains a uniform absolute velocity.

In the atmosphere, motions are nearly always generated and maintained by pressure gradient forces; the conditions of uniform pressure required for pure inertial flow rarely exist. In the oceans, however, currents are often generated by transient winds blowing across the surface, rather than by internal pressure gradients. As a result, significant amounts of energy occur in currents that oscillate with near inertial periods. An example recorded by a current meter near the island of Barbados is shown in Figure 3.3.

3.2.4 Cyclostrophic Flow

If the horizontal scale of a disturbance is small enough, the Coriolis force may be neglected in (3.10) compared to the pressure gradient force and the centrifugal force. The force balance normal to the direction of flow is then

$$\frac{V^2}{R} = -\frac{\partial \Phi}{\partial n}$$

If this equation is solved for V, we obtain the speed of the *cyclostrophic wind*

$$V = \left(-R\frac{\partial \Phi}{\partial n}\right)^{1/2} \tag{3.14}$$

As indicated in Figure 3.4, cyclostrophic flow may be either cyclonic or anticyclonic. In both cases the pressure gradient force is directed toward the center of curvature and the centrifugal force away from the center of curvature.

The cyclostrophic balance approximation is valid provided that the ratio of the centrifugal force to the Coriolis force is large. This ratio $V/(fR)$ is equivalent to the Rossby number discussed in Section 2.4.2. As an example of cyclostrophic scale motion, we consider a typical tornado. Suppose that the tangential velocity is 30 m s^{-1} at a distance of 300 m from the center of the vortex.

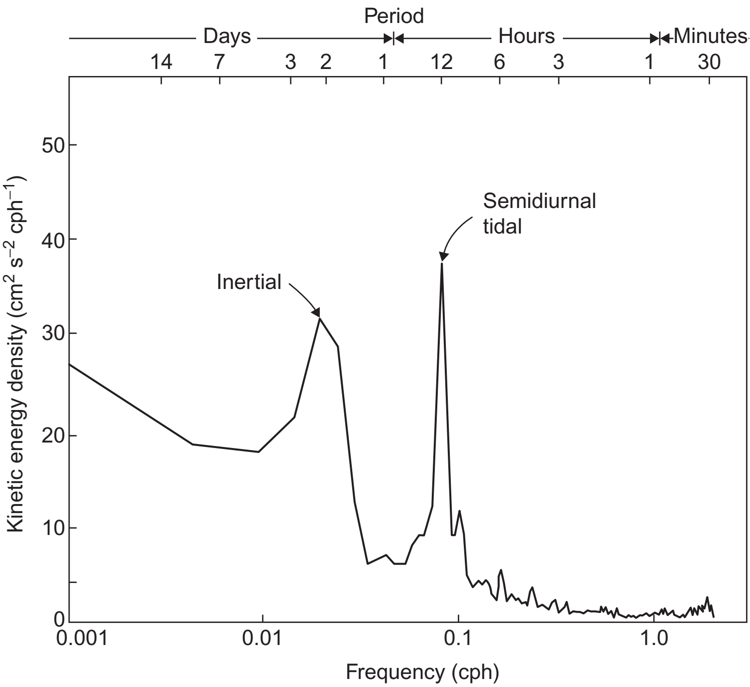

FIGURE 3.3 Power spectrum of kinetic energy at 30-m depth in the ocean near Barbados (13°N). Ordinate shows kinetic energy density per unit frequency interval (cph^{-1} designates cycles per hour). This type of plot indicates the manner in which the total kinetic energy is partitioned among oscillations of different periods. Note the strong peak at 53 h, which is the period of an inertial oscillation at 13° latitude. (*After Warsh et al., 1971. Copyright © American Meteorological Society. Reprinted with permission.*)

Assuming that $f = 10^{-4}\ \text{s}^{-1}$, the Rossby number is just $\text{Ro} = V/|fR| \approx 10^3$, which implies that the Coriolis force can be neglected in computing the balance of forces for a tornado. However, the majority of tornadoes in the Northern Hemisphere are observed to rotate in a cyclonic (counterclockwise) sense. This is due to the fact that they are embedded in environments that favor cyclonic rotation (see Section 9.6.1). Smaller-scale vortices, however, such as dust devils and water spouts, do not have a preferred direction of rotation. According to data collected by Sinclair (1965), they are observed to be anticyclonic as often as cyclonic.

3.2.5 The Gradient Wind Approximation

Horizontal frictionless flow that is parallel to the height contours so that the tangential acceleration vanishes ($DV/Dt = 0$) is called *gradient flow*. Gradient flow is a three-way balance among the Coriolis force, the centrifugal force, and the horizontal pressure gradient force. Like geostrophic flow, pure gradient flow

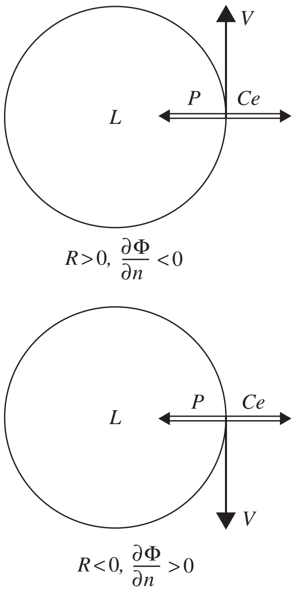

FIGURE 3.4 Force balance in cyclostrophic flow: P designates the pressure gradient; Ce designates the centrifugal force.

can exist only under very special circumstances. It is always possible, however, to define a gradient wind, which at any point is just the wind component parallel to the height contours that satisfies (3.10). For this reason, (3.10) is commonly referred to as the gradient wind equation. Because (3.10) takes into account the centrifugal force due to the curvature of parcel trajectories, the gradient wind is often a better approximation to the actual wind than the geostrophic wind.

The gradient wind speed is obtained by solving (3.10) for V to yield

$$\begin{aligned} V &= -\frac{fR}{2} \pm \left(\frac{f^2R^2}{4} - R\frac{\partial\Phi}{\partial n}\right)^{1/2} \\ &= -\frac{fR}{2} \pm \left(\frac{f^2R^2}{4} + fRV_g\right)^{1/2} \end{aligned} \tag{3.15}$$

where in the lower expression (3.11) is used to express $\partial\Phi/\partial n$ in terms of the geostrophic wind. Not all the mathematically possible roots of (3.15) correspond to physically possible solutions, since it is required that V be real and nonnegative. In Table 3.1 the various roots of (3.15) are classified according to the signs of R and $\partial\Phi/\partial n$ in order to isolate the physically meaningful solutions.

The force balances for the four permitted solutions are illustrated in Figure 3.5. Equation (3.15) shows that in cases of both regular and anomalous highs the pressure gradient is limited by the requirement that the quantity under

TABLE 3.1 Classification of Roots of the Gradient Wind Equation in the Northern Hemisphere

Sign $\partial\Phi/\partial n$	$R > 0$	$R < 0$
Positive ($V_g < 0$)	Positive root[a]: unphysical	Positive root: antibaric flow (anomalous low)
	Negative root: unphysical	Negative root: unphysical
Negative ($V_g > 0$)	Positive root: cyclonic flow (regular low)	Positive root: ($V > -fR/2$): anticyclonic flow (anomalous high)
	Negative root: unphysical	Negative root: ($V < -fR/2$): anticyclonic flow (regular high)

[a] *The terms "positive root" and "negative root" in columns 2 and 3 refer to the sign taken in the final term in Eq. (3.15).*

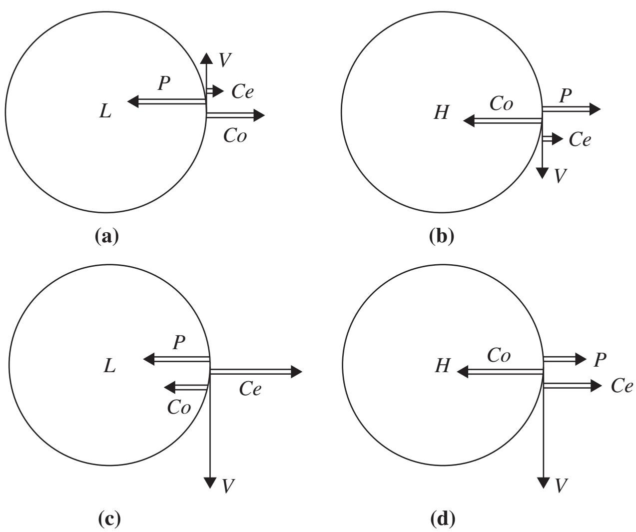

FIGURE 3.5 Force balances in the Northern Hemisphere for the four types of gradient flow: (a) regular low, (b) regular high, (c) anomalous low, and (d) anomalous high.

the radical be nonnegative—that is,

$$\left| f V_g \right| = \left| \frac{\partial \Phi}{\partial n} \right| < \frac{|R| f^2}{4} \tag{3.16}$$

Thus, the pressure gradient in a high must approach zero as $|R| \to 0$. It is for this reason that the pressure field near the center of a high is always flat and the wind gentle compared to the region near the center of a low.

The absolute angular momentum about the axis of rotation for the circularly symmetric motions shown in Figure 3.5 is given by $VR + fR^2/2$. From (3.15) it is verified readily that regular gradient wind balances have positive absolute angular momentum in the Northern Hemisphere, whereas anomalous cases have negative absolute angular momentum. Because the only source of negative absolute angular momentum is the Southern Hemisphere, the anomalous cases are unlikely to occur, except perhaps close to the equator.

In all cases except the anomalous low (Figure 3.5c) the horizontal components of the Coriolis and pressure gradient forces are oppositely directed. Such flow is called *baric*. The anomalous low is antibaric; the geostrophic wind V_g defined in (3.11) is negative for an anomalous low and is clearly not a useful approximation to the actual speed.[4] Furthermore, as shown in Figure 3.5, gradient flow is cyclonic only when the centrifugal force and the horizontal component of the Coriolis force have the same sense ($Rf > 0$); it is anticyclonic when these forces have the opposite sense ($Rf < 0$). Since the direction of anticyclonic and cyclonic flow is reversed in the Southern Hemisphere, the requirement that $Rf > 0$ for cyclonic flow holds regardless of the hemisphere considered.

The definition of the geostrophic wind (3.11) can be used to rewrite the force balance normal to the direction of flow (3.10) in the form

$$V^2/R + fV - fV_g = 0$$

Dividing through by fV shows that the ratio of the geostrophic wind to the gradient wind is

$$\frac{V_g}{V} = 1 + \frac{V}{fR} \tag{3.17}$$

For normal cyclonic flow ($fR > 0$), V_g is larger than V, whereas for anticyclonic flow ($fR < 0$), V_g is smaller than V. Therefore, the geostrophic wind is an overestimate of the balanced wind in a region of cyclonic curvature and an underestimate in a region of anticyclonic curvature. For midlatitude synoptic systems, the difference between gradient and geostrophic wind speeds generally does not exceed 10 to 20%. [Note that the magnitude of $V/(fR)$ is just the Rossby number.] For tropical disturbances, the Rossby number is in the range of 1 to 10, and the gradient wind formula must be applied rather than the geostrophic wind. Equation (3.17) also shows that the antibaric anomalous low, which has $V_g < 0$, can exist only when $V/(fR) < -1$. Thus, antibaric flow is associated with small-scale intense vortices such as tornadoes.

---

[4] Remember that in the natural coordinate system the speed V is positive definite.

3.3 TRAJECTORIES AND STREAMLINES

In the natural coordinate system used in the previous section to discuss balanced flow, $s(x, y, t)$ was defined as the distance along the curve in the horizontal plane traced out by the path of an air parcel. The path followed by a particular air parcel over a finite period of time is called the *trajectory* of the parcel. Thus, the radius of curvature R of the path s referred to in the gradient wind equation is the radius of curvature for a parcel trajectory. In practice, R is often estimated by using the radius of curvature of a geopotential height contour, as this can be estimated easily from a synoptic chart. However, the height contours are actually *streamlines* of the gradient wind (i.e., lines that are everywhere parallel to the instantaneous wind velocity).

It is important to distinguish clearly between streamlines, which give a "snapshot" of the velocity field at any instant, and trajectories, which trace the motion of individual fluid parcels over a finite time interval. In Cartesian coordinates, horizontal trajectories are determined by the integration of

$$\frac{Ds}{Dt} = V(x, y, t) \tag{3.18}$$

over a finite time span for each parcel to be followed, whereas streamlines are determined by the integration of

$$\frac{dy}{dx} = \frac{v(x, y, t_0)}{u(x, y, t_0)} \tag{3.19}$$

with respect to x at time t_0. (Note that since a streamline is parallel to the velocity field, its slope in the horizontal plane is just the ratio of the horizontal velocity components.) Only for *steady-state* motion fields (i.e., fields in which the local rate of change of velocity vanishes) do the streamlines and trajectories coincide. However, synoptic disturbances are not steady-state motions. They generally move at speeds of the same order as the winds that circulate about them. To gain an appreciation for the possible errors involved in using the curvature of the streamlines instead of the curvature of the trajectories in the gradient wind equation, it is necessary to investigate the relationship between the curvature of the trajectories and the curvature of the streamlines for a moving pressure system.

We let $\beta(x, y, t)$ designate the angular direction of the wind at each point on an isobaric surface, and R_t and R_s designate the radii of curvature of the trajectories and streamlines, respectively. Then, from Figure 3.6, $\delta s = R\, \delta\beta$ so that in the limit $\delta s \to 0$

$$\frac{D\beta}{Ds} = \frac{1}{R_t} \quad \text{and} \quad \frac{\partial\beta}{\partial s} = \frac{1}{R_s} \tag{3.20}$$

where $D\beta/Ds$ means the rate of change of wind direction along a trajectory (positive for counterclockwise turning) and $\partial\beta/\partial s$ is the rate of change of wind

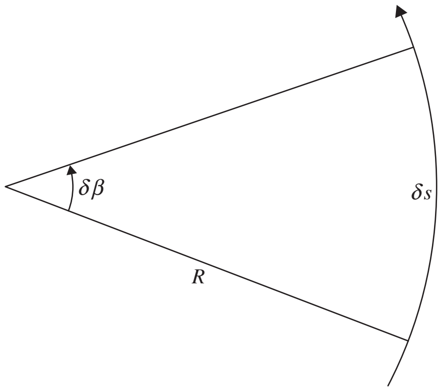

FIGURE 3.6 Relationship between the change in angular direction of the wind $\delta\beta$ and the radius of curvature R.

direction along a streamline at any instant. Thus, the rate of change of wind direction following the motion is

$$\frac{D\beta}{Dt} = \frac{D\beta}{Ds}\frac{Ds}{Dt} = \frac{V}{R_t} \tag{3.21}$$

or, after expanding the total derivative,

$$\frac{D\beta}{Dt} = \frac{\partial\beta}{\partial t} + V\frac{\partial\beta}{\partial s} = \frac{\partial\beta}{\partial t} + \frac{V}{R_s} \tag{3.22}$$

Combining (3.21) and (3.22), we obtain a formula for the local turning of the wind:

$$\frac{\partial\beta}{\partial t} = V\left(\frac{1}{R_t} - \frac{1}{R_s}\right) \tag{3.23}$$

Equation (3.23) indicates that the trajectories and streamlines will coincide only when the local rate of change of the wind direction vanishes.

In general, midlatitude synoptic systems move eastward as a result of advection by upper-level westerly winds. In such cases there is a local turning of the wind due to the motion of the system even if the shape of the height contour pattern remains constant as the system moves. The relationship between R_t and R_s in such a situation can be determined easily for an idealized circular pattern of height contours moving at a constant velocity **C**. In this case the local turning of the wind is entirely due to the motion of the streamline pattern so that

$$\frac{\partial\beta}{\partial t} = -\mathbf{C}\cdot\nabla\beta = -C\frac{\partial\beta}{\partial s}\cos\gamma = -\frac{C}{R_s}\cos\gamma$$

where γ is the angle between the streamlines (height contours) and the direction of motion of the system. Substituting the preceding equation into (3.23) and solving for R_t with the aid of (3.20), we obtain the desired relationship between the curvature of the streamlines and the curvature of the trajectories:

$$R_t = R_s\left(1 - \frac{C\cos\gamma}{V}\right)^{-1} \tag{3.24}$$

Equation (3.24) can be used to compute the curvature of the trajectory anywhere on a moving pattern of streamlines. In Figure 3.7 the curvatures of the trajectories for parcels initially located due north, east, south, and west of the center of a cyclonic system are shown both for the case of a wind speed greater than the speed of movement of the height contours and for the case of a wind speed less than the speed of movement of the height contours. In these examples the plotted trajectories are based on a geostrophic balance so that the height

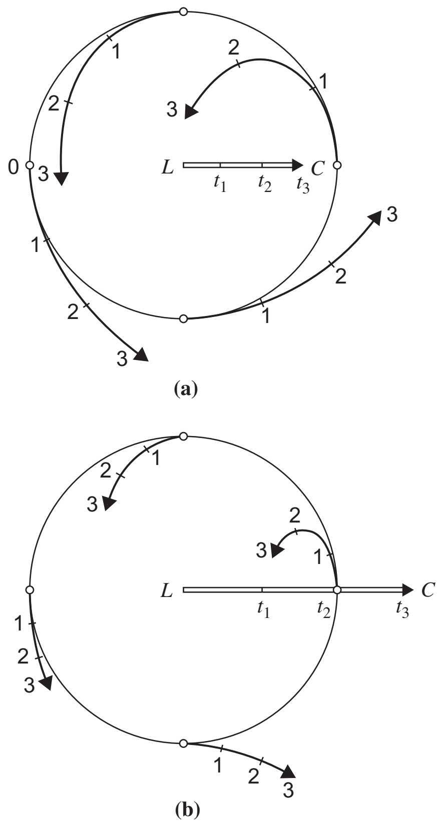

FIGURE 3.7 Trajectories for moving circular cyclonic circulation systems in the Northern Hemisphere with (a) $V = 2C$ and (b) $2V = C$. Numbers indicate positions at successive times. L designates a pressure minimum.

contours are equivalent to streamlines. It is also assumed for simplicity that the wind speed does not depend on the distance from the center of the system.

In the case shown in Figure 3.7b, there is a region south of the low center where the curvature of the trajectories is opposite that of the streamlines. Because synoptic-scale pressure systems usually move at speeds comparable to the wind speed, the gradient wind speed computed on the basis of the curvature of the height contours is often no better an approximation to the actual wind speed than the geostrophic wind. In fact, the actual gradient wind speed will vary along a height contour with the variation of the trajectory curvature.

3.4 THE THERMAL WIND

The geostrophic wind must have vertical shear in the presence of a horizontal temperature gradient, as can be shown easily from simple physical considerations based on hydrostatic equilibrium. Since the geostrophic wind (3.4) is proportional to the geopotential gradient on an isobaric surface, a geostrophic wind directed along the positive y axis that increases in magnitude with height requires that the slope of the isobaric surfaces with respect to the x axis also must increase with height, as shown in Figure 3.8. According to the hypsometric equation (1.30), the thickness δz corresponding to a (positive) pressure interval δp is

$$\delta z \approx g^{-1} RT \delta \ln p \tag{3.25}$$

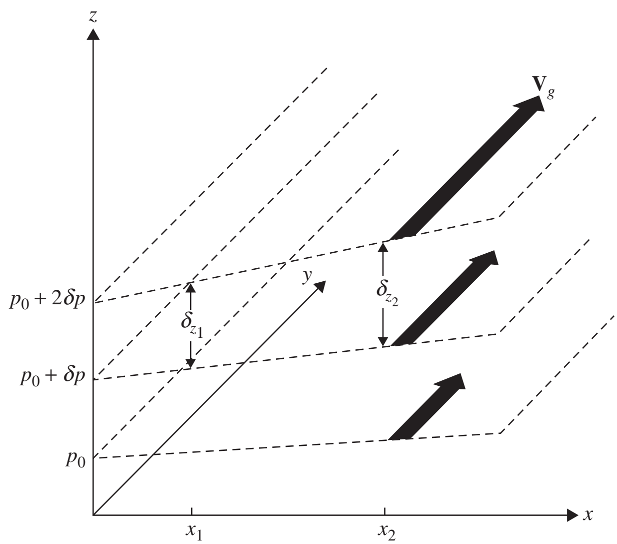

FIGURE 3.8 Relationship between vertical shear of the geostrophic wind and horizontal thickness gradients. (Note that $\delta p < 0$.)

Thus, the thickness of the layer between two isobaric surfaces is proportional to the mean temperature in the layer, T. In Figure 3.8 the mean temperature T_1 of the column denoted δz_1 must be less than the mean temperature T_2 for the column denoted δz_2. Thus, an increase with height of a positive x directed pressure gradient must be associated with a positive x directed temperature gradient. The air in a vertical column at x_2, because it is warmer (less dense), must occupy a greater depth for a given pressure drop than the air at x_1.

Equations for the rate of change with height of the geostrophic wind components are derived most easily using the isobaric coordinate system. In isobaric coordinates the geostrophic wind (3.4) has components given by

$$v_g = \frac{1}{f}\frac{\partial \Phi}{\partial x} \quad \text{and} \quad u_g = -\frac{1}{f}\frac{\partial \Phi}{\partial y} \tag{3.26}$$

where the derivatives are evaluated with pressure held constant. Also, with the aid of the ideal gas law, we can write the hydrostatic equation as

$$\frac{\partial \Phi}{\partial p} = -\alpha = -\frac{RT}{p} \tag{3.27}$$

Differentiating (3.26) with respect to pressure, and applying (3.27), we obtain

$$p\frac{\partial v_g}{\partial p} \equiv \frac{\partial v_g}{\partial \ln p} = -\frac{R}{f}\left(\frac{\partial T}{\partial x}\right)_p \tag{3.28}$$

$$p\frac{\partial u_g}{\partial p} \equiv \frac{\partial u_g}{\partial \ln p} = \frac{R}{f}\left(\frac{\partial T}{\partial y}\right)_p \tag{3.29}$$

or in vectorial form

$$\frac{\partial \mathbf{V}_g}{\partial \ln p} = -\frac{R}{f}\mathbf{k} \times \nabla_p T \tag{3.30}$$

Equation (3.30) is often referred to as the *thermal wind* equation. However, it is actually a relationship for the vertical wind *shear* (i.e., the rate of change of the geostrophic wind with respect to $\ln p$). Strictly speaking, the term *thermal wind* refers to the vector difference between geostrophic winds at two levels. Designating the thermal wind vector by $\mathbf{V}_T$, we may integrate (3.30) from pressure level p_0 to level p_1 $(p_1 < p_0)$ to get

$$\mathbf{V}_T \equiv \mathbf{V}_g(p_1) - \mathbf{V}_g(p_0) = -\frac{R}{f}\int_{p_0}^{p_1} \left(\mathbf{k} \times \nabla_p T\right) d\ln p \tag{3.31}$$

Letting $\langle T \rangle$ denote the mean temperature in the layer between pressure p_0 and p_1, the x and y components of the thermal wind are thus given by

$$u_T = -\frac{R}{f}\left(\frac{\partial \langle T \rangle}{\partial y}\right)_p \ln\left(\frac{p_0}{p_1}\right); \quad v_T = \frac{R}{f}\left(\frac{\partial \langle T \rangle}{\partial x}\right)_p \ln\left(\frac{p_0}{p_1}\right) \tag{3.32}$$

Alternatively, we may express the thermal wind for a given layer in terms of the horizontal gradient of the geopotential difference between the top and the bottom of the layer:

$$u_T = -\frac{1}{f}\frac{\partial}{\partial y}(\Phi_1 - \Phi_0); \quad v_T = \frac{1}{f}\frac{\partial}{\partial x}(\Phi_1 - \Phi_0) \tag{3.33}$$

The equivalence of (3.32) and (3.33) can be verified readily by integrating the hydrostatic equation (3.27) vertically from p_0 to p_1 after replacing T by the mean $\langle T \rangle$. The result is the hypsometric equation (1.29):

$$\Phi_1 - \Phi_0 \equiv gZ_T = R\langle T \rangle \ln\left(\frac{p_0}{p_1}\right) \tag{3.34}$$

The quantity Z_T is the *thickness* of the layer between p_0 and p_1 measured in units of geopotential meters. From (3.34) we see that the thickness is proportional to the mean temperature in the layer. Hence, lines of equal Z_T (isolines of thickness) are equivalent to the isotherms of mean temperature in the layer. It can also be used to estimate the mean horizontal temperature advection in a layer, as shown in Figure 3.9. It is clear from the vector form of the thermal

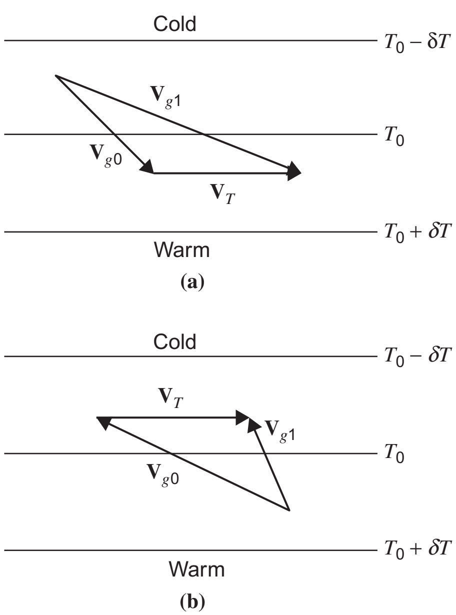

FIGURE 3.9 Relationship between turning of geostrophic wind and temperature advection: (a) backing of the wind with height and (b) veering of the wind with height.

wind relation

$$\mathbf{V}_T = \frac{1}{f}\mathbf{k} \times \nabla (\Phi_1 - \Phi_0) = \frac{g}{f}\mathbf{k} \times \nabla Z_T = \frac{R}{f}\mathbf{k} \times \nabla \langle T \rangle \ln \left(\frac{p_0}{p_1}\right) \qquad (3.35)$$

that the thermal wind blows parallel to the isotherms (lines of constant thickness) with the warm air to the right facing downstream in the Northern Hemisphere. Thus, as is illustrated in Figure 3.9a, a geostrophic wind that turns counterclockwise with height (backs) is associated with cold-air advection. Conversely, as shown in Figure 3.9b, clockwise turning (veering) of the geostrophic wind with height implies warm advection by the geostrophic wind in the layer.

It is therefore possible to obtain a reasonable estimate of the horizontal temperature advection and its vertical dependence at a given location solely from data on the vertical profile of the wind given by a single sounding. Alternatively, the geostrophic wind at any level can be estimated from the mean temperature field, provided that the geostrophic velocity is known at a single level. Thus, for example, if the geostrophic wind at 850 hPa is known and the mean horizontal temperature gradient in the layer 850 to 500 hPa is also known, the thermal wind equation can be applied to obtain the geostrophic wind at 500 hPa.

3.4.1 Barotropic and Baroclinic Atmospheres

A *barotropic* atmosphere is one in which the density depends only on the pressure, $\rho = \rho(p)$, so that isobaric surfaces are also surfaces of constant density. For an ideal gas, the isobaric surfaces will also be isothermal if the atmosphere is barotropic. Thus, $\nabla_p T = 0$ in a barotropic atmosphere, and the thermal wind equation (3.30) becomes $\partial \mathbf{V}_g / \partial \ln p = 0$, which states that the geostrophic wind is independent of height in a barotropic atmosphere. Thus, barotropy provides a very strong constraint on the motions in a rotating fluid; the large-scale motion can depend only on horizontal position and time, not on height.

An atmosphere in which density depends on both the temperature and the pressure, $\rho = \rho\,(p, T)$, is referred to as a *baroclinic* atmosphere. In a baroclinic atmosphere the geostrophic wind generally has vertical shear, and this shear is related to the horizontal temperature gradient by the thermal wind equation (3.30). Obviously, the baroclinic atmosphere is of primary importance in dynamic meteorology. However, as shown in later chapters, much can be learned by study of the simpler barotropic atmosphere.

3.5 VERTICAL MOTION

As mentioned previously, for synoptic-scale motions the vertical velocity component is typically of the order of a few centimeters per second. Routine meteorological soundings, however, only give the wind speed to an accuracy of about a meter per second. Thus, in general the vertical velocity is not measured directly but must be inferred from the fields that are measured directly.

Two methods for inferring the vertical motion field are the kinematic method, based on the equation of continuity, and the adiabatic method, based on the thermodynamic energy equation. Both methods are usually applied using the isobaric coordinate system so that $\omega(p)$ is inferred rather than $w(z)$. These two measures of vertical motion can be related to each other with the aid of the hydrostatic approximation.

Expanding Dp/Dt in the (x, y, z) coordinate system yields

$$\omega \equiv \frac{Dp}{Dt} = \frac{\partial p}{\partial t} + \mathbf{V} \cdot \nabla p + w\left(\frac{\partial p}{\partial z}\right) \tag{3.36}$$

Now, for synoptic-scale motions, the horizontal velocity is geostrophic to a first approximation. Therefore, we can write $\mathbf{V} = \mathbf{V}_g + \mathbf{V}_a$, where $\mathbf{V}_a$ is the *ageostrophic* wind and $|\mathbf{V}_a| \ll |\mathbf{V}_g|$. However, $\mathbf{V}_g = (\rho f)^{-1}\mathbf{k} \times \nabla p$, so that $\mathbf{V}_g \cdot \nabla p = 0$. Using this result plus the hydrostatic approximation, (3.36) may be rewritten as

$$\omega = \frac{\partial p}{\partial t} + \mathbf{V}_a \cdot \nabla p - g\rho w \tag{3.37}$$

Comparing the magnitudes of the three terms on the right in (3.37), we find that for synoptic-scale motions

$$\partial p/\partial t \sim 10 \text{ hPa d}^{-1}$$
$$\mathbf{V}_a \cdot \nabla p \sim \left(1 \text{ m s}^{-1}\right)\left(1 \text{ Pa km}^{-1}\right) \sim 1 \text{ hPa d}^{-1}$$
$$g\rho w \sim 100 \text{ hPa d}^{-1}$$

Thus, it is quite a good approximation to let

$$\omega = -\rho g w \tag{3.38}$$

3.5.1 The Kinematic Method

One method of deducing the vertical velocity is based on integrating the continuity equation in the vertical. Integration of (3.5) with respect to pressure from a reference level p_s to any level p yields

$$\begin{aligned} \omega(p) &= \omega(p_s) - \int_{p_s}^{p} \left(\frac{\partial u}{\partial x} + \frac{\partial v}{\partial y}\right)_p dp \\ &= \omega(p_s) + (p_s - p)\left(\frac{\partial \langle u \rangle}{\partial x} + \frac{\partial \langle v \rangle}{\partial y}\right)_p \end{aligned} \tag{3.39}$$

Here the angle brackets denote a pressure-weighted vertical average:

$$\langle\ \rangle \equiv (p - p_s)^{-1} \int_{p_s}^{p} ()dp$$

With the aid of (3.38), the averaged form of (3.39) can be rewritten as

$$w(z) = \frac{\rho\,(z_s)\,w\,(z_s)}{\rho(z)} - \frac{p_s - p}{\rho(z)g}\left(\frac{\partial\,\langle u\rangle}{\partial x} + \frac{\partial\,\langle v\rangle}{\partial y}\right) \tag{3.40}$$

where z and z_s are the heights of pressure levels p and p_s, respectively.

Application of (3.40) to infer the vertical velocity field requires knowledge of the horizontal divergence. To determine the horizontal divergence, the partial derivatives $\partial u/\partial x$ and $\partial v/\partial y$ are generally estimated from the fields of u and v by using *finite difference* approximations (see Section 13.2.1). For example, to determine the divergence of the horizontal velocity at the point x_0, y_0 in Figure 3.10, we write

$$\frac{\partial u}{\partial x} + \frac{\partial v}{\partial y} \approx \frac{u\,(x_0 + d) - u\,(x_0 - d)}{2d} + \frac{v\,(y_0 + d) - v\,(y_0 - d)}{2d} \tag{3.41}$$

However, for synoptic-scale motions in midlatitudes, the horizontal velocity is nearly in geostrophic equilibrium. Except for the small effect due to the variation of the Coriolis parameter (see Problem 3.19), the geostrophic wind is nondivergent; that is, $\partial u/\partial x$ and $\partial v/\partial y$ are nearly equal in magnitude but opposite in sign. Thus, the horizontal divergence is due primarily to the small departures of the wind from geostrophic balance (i.e., the ageostrophic wind). A 10% error in evaluating one of the wind components in (3.41) can easily cause the estimated divergence to be in error by 100%. For this reason, the continuity equation method is not recommended for estimating the vertical motion field from observed horizontal winds.

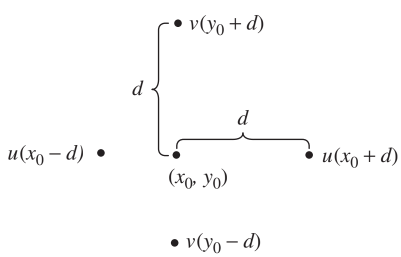

FIGURE 3.10 Grid for estimation of the horizontal divergence.

3.5.2 The Adiabatic Method

A second method for inferring vertical velocities, which is not so sensitive to errors in the measured horizontal velocities, is based on the thermodynamic energy equation. If the diabatic heating J is small compared to the other terms in the heat balance, (3.6) yields

$$\omega = S_p^{-1}\left(\frac{\partial T}{\partial t} + u\frac{\partial T}{\partial x} + v\frac{\partial T}{\partial y}\right) \tag{3.42}$$

Because temperature advection can usually be estimated quite accurately in midlatitudes by using geostrophic winds, the adiabatic method can be applied when only geopotential and temperature data are available. A disadvantage of the adiabatic method is that the local rate of change of temperature is required. Unless observations are taken at close intervals in time, it may be difficult to accurately estimate $\partial T/\partial t$ over a wide area. This method is also rather inaccurate in situations where strong diabatic heating is present, such as storms in which heavy rainfall occurs over a large area. Chapter 6 presents an alternative method for estimating ω, based on the so-called *omega equation*, that does not suffer from these difficulties.

3.6 SURFACE PRESSURE TENDENCY

The development of a negative surface *pressure tendency* is a classic warning of an approaching cyclonic weather disturbance. A simple expression that relates the surface pressure tendency to the wind field, and thus in theory might be used as the basis for short-range forecasts, can be obtained by taking the limit $p \to 0$ in (3.39) to get

$$\omega(p_s) = -\int_0^{p_s} (\nabla \cdot \mathbf{V})\, dp \tag{3.43}$$

followed by substituting from (3.37) to yield

$$\frac{\partial p_s}{\partial t} \approx -\int_0^{p_s} (\nabla \cdot \mathbf{V})\, dp \tag{3.44}$$

Here we have assumed that the surface is horizontal so that $w_s = 0$, and have neglected advection by the ageostrophic surface velocity in accord with the scaling arguments in Section 3.5.1.

According to (3.44), the surface pressure tendency at a given point is determined by the total convergence of mass into the vertical column of atmosphere above that point. This result is a direct consequence of the hydrostatic assumption, which implies that the pressure at a point is determined solely by the weight of the column of air above that point. Temperature changes in the air column will affect the heights of upper-level pressure surfaces, but not the surface pressure.

Although, as stated earlier, the tendency equation might appear to have potential as a forecasting aid, its utility is severely limited due to the fact that, as discussed in Section 3.5.1, $\nabla \cdot \mathbf{V}$ is difficult to compute accurately from observations because it depends on the ageostrophic wind field. In addition, there is a strong tendency for vertical compensation. Thus, when there is convergence in the lower troposphere, there is divergence aloft, and vice versa. The net integrated convergence or divergence is then a small residual in the vertical integral of a poorly determined quantity.

Nevertheless, (3.44) does have qualitative value as an aid in understanding the origin of surface pressure changes and the relationship of such changes to the horizontal divergence. This can be illustrated by considering (as one possible example) the development of a thermal cyclone. We suppose that a heat source generates a local warm anomaly in the midtroposphere (Figure 3.11a). Then, according to the hypsometric equation (3.34), the heights of the upper-level pressure surfaces are raised above the warm anomaly, resulting in a horizontal pressure gradient force at the upper levels, which drives a divergent upper-level wind. By (3.44) this upper-level divergence will initially cause the surface pressure to decrease, thus generating a surface low below the warm anomaly (Figure 3.11b). The horizontal pressure gradient associated with the surface low then drives a low-level convergence and vertical circulation, which tends to compensate the upper-level divergence. The degree of compensation between upper divergence and lower convergence will determine whether the surface pressure continues to fall, remains steady, or rises.

The thermally driven circulation of the preceding example is by no means the only type of circulation possible (e.g., cold-core cyclones are important synoptic-scale features). However, it does provide insight into how dynamical processes at upper levels are communicated to the surface and how the

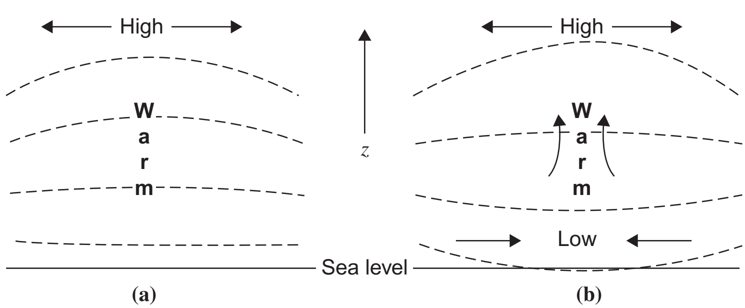

FIGURE 3.11 Adjustment of surface pressure to a midtropospheric heat source. *Dashed lines* indicate isobars. (a) Initial height increase at upper-level pressure surface. (b) Surface response to upper-level divergence.

surface and upper troposphere are dynamically connected through the divergent circulation. This subject is considered in detail in Chapter 6.

Equation (3.44) is a lower boundary condition that determines the evolution of pressure at constant height. If the isobaric coordinate system of dynamical equations (3.2), (3.5), (3.6), and (3.27) is used as the set of governing equations, the lower boundary condition should be expressed in terms of the evolution of geopotential (or geopotential height) at constant pressure. Such an expression can be obtained simply by expanding $D\Phi/Dt$ in isobaric coordinates

$$\frac{\partial \Phi}{\partial t} = -\mathbf{V}_a \cdot \nabla \Phi - \omega \frac{\partial \Phi}{\partial p}$$

and substituting from (3.27) and (3.43) to get

$$\frac{\partial \Phi_s}{\partial t} \approx -\frac{RT_s}{p_s} \int_0^{p_s} (\nabla \cdot \mathbf{V})\, dp \tag{3.45}$$

where we have again neglected advection by the ageostrophic wind.

In practice, the boundary condition (3.45) is difficult to use because it should be applied at pressure p_s, which is itself changing in time and space. In simple models it is usual to assume that p_s is constant (usually 1000 hPa) and to let $\omega = 0$ at p_s. For modern forecast models, an alternative coordinate system is generally employed in which the lower boundary is always a coordinate surface. This approach is described in Section 10.3.1.

PROBLEMS

3.1. An aircraft flying a heading of 60° (i.e., 60° to the east of north) at air speed 200 m s^{-1} moves relative to the ground due east (90°) at 225 m s^{-1}. If the plane is flying at constant pressure, what is its rate of change in altitude (in meters per kilometer horizontal distance) assuming a steady pressure field, geostrophic winds, and $f = 10^{-4}\,\mathrm{s}^{-1}$?

3.2. The actual wind is directed 30° to the right of the geostrophic wind. If the geostrophic wind is 20 m s^{-1}, what is the rate of change of wind speed? Let $f = 10^{-4}\,\mathrm{s}^{-1}$.

3.3. A tornado rotates with constant angular velocity ω. Show that the surface pressure at the center of the tornado is given by

$$p = p_0 \exp\left(\frac{-\omega^2 r_0^2}{2RT}\right)$$

where p_0 is the surface pressure at a distance r_0 from the center and T is the temperature (assumed constant). If the temperature is 288 K and pressure and wind speed at 100 m from the center are 1000 hPa and 100 m s^{-1}, respectively, what is the central pressure?

3.4. Calculate the geostrophic wind speed (m s^{-1}) on an isobaric surface for a geopotential height gradient of 100 m per 1000 km, and compare with all possible gradient wind speeds for the same geopotential height gradient and a radius of curvature of $\pm$ 500 km. Let $f = 10^{-4}\ s^{-1}$.

3.5. Determine the maximum possible ratio of the normal anticyclonic gradient wind speed to the geostrophic wind speed for the same pressure gradient.

3.6. Show that the geostrophic balance in isothermal coordinates may be written

$$f\mathbf{V}_g = \mathbf{k} \times \nabla_T (RT \ln p + \Phi)$$

3.7. Determine the radii of curvature for the trajectories of air parcels located 500 km to the east, north, south, and west of the center of a circular low-pressure system, respectively. The system is moving eastward at 15 m s^{-1}. Assume geostrophic flow with a uniform tangential wind speed of 15 m s^{-1}.

3.8. Determine the normal gradient wind speeds for the four air parcels of Problem 3.7. Using the radii of curvature computed in the previous problem, compare these speeds with the geostrophic speed. (Let $f = 10^{-4}\ s^{-1}$.) Use the gradient wind speeds calculated here to recompute the radii of curvature for the four air parcels referred to in Problem 3.7. Use these new estimates of the radii of curvature to recompute the gradient wind speeds for the four air parcels. What fractional error is made in the radii of curvature by using the geostrophic wind approximation in this case? [Note that further iterations could be carried out but would converge rapidly.]

3.9. Show that as the pressure gradient approaches zero, the gradient wind reduces to the geostrophic wind for a normal anticyclone and to inertial flow (Section 3.2.3) for an anomalous anticyclone.

3.10. The mean temperature in the layer between 750 and 500 hPa decreases eastward by 3°C per 100 km. If the 750-hPa geostrophic wind is from the southeast at 20 m s^{-1}, what is the geostrophic wind speed and direction at 500 hPa? Let $f = 10^{-4}\ s^{-1}$.

3.11. What is the mean temperature advection in the 750- to 500-hPa layer in Problem 3.10?

3.12. Suppose that a vertical column of the atmosphere at 43°N is initially isothermal from 900 to 500 hPa. The geostrophic wind is 10 m s^{-1} from the south at 900 hPa, 10 m s^{-1} from the west at 700 hPa, and 20 m s^{-1} from the west at 500 hPa. Calculate the mean horizontal temperature gradients in the two layers 900 to 700 hPa and 700 to 500 hPa. Compute the rate of advective temperature change in each layer. How long would this advection pattern have to persist in order to establish a dry adiabatic lapse rate between 600 and 800 hPa? (Assume that the lapse rate is constant between 900 and 500 hPa and that the 800- to 600-hPa layer thickness is 2.25 km.)

3.13. An airplane pilot crossing the ocean at 45°N latitude has both a pressure altimeter and a radar altimeter, the latter measuring his absolute height above the sea. Flying at an air speed of 100 m s^{-1}, he maintains altitude by referring to his pressure altimeter set for a sea-level pressure of 1013 hPa. He holds an indicated 6000-m altitude. At the beginning of a 1-h period he notes that his radar altimeter reads 5700 m, and at the end of the hour he notes that it reads 5950 m. In what direction and approximately how far has he drifted from his heading?

3.14. Work out a gradient wind classification scheme equivalent to Table 3.1 for the Southern Hemisphere (f¡0) case.

3.15. In the geostrophic momentum approximation (Hoskins, 1975) the gradient wind formula for steady circular flow (3.17) is replaced by the approximation

$$VV_g R^{-1} + fV = fV_g$$

Compare the speeds V computed using this approximation with those obtained in Problem 3.8 using the gradient wind formula.

3.16. How large can the ratio $V_g/(fR)$ be before the geostrophic momentum approximation differs from the gradient wind approximation by 10% for cyclonic flow?

3.17. The planet Venus rotates about its axis so slowly that to a reasonable approximation the Coriolis parameter may be set equal to zero. For steady, frictionless motion parallel to latitude circles, the momentum equation (2.20) then reduces to a type of cyclostrophic balance:

$$\frac{u^2 \tan\phi}{a} = -\frac{1}{\rho}\frac{\partial p}{\partial y}$$

By transforming this expression to isobaric coordinates, show that the thermal wind equation in this case can be expressed in the form

$$\omega_r^2(p_1) - \omega_r^2(p_0) = \frac{-R\ln(p_0/p_1)}{(a\sin\phi\cos\phi)}\frac{\partial\langle T\rangle}{\partial y}$$

where R is the gas constant, a is the radius of the planet, and $\omega_r \equiv u/(a\cos\phi)$ is the relative angular velocity. How must $\langle T\rangle$ (the vertically averaged temperature) vary with respect to latitude in order for ω_r to be a function only of pressure? If the zonal velocity at about 60 km above the equator ($p_1 = 2.9 \times 10^5$ Pa) is 100 m s^{-1} and the zonal velocity vanishes at the surface of the planet ($p_0 = 9.5 \times 10^6$ Pa), what is the vertically averaged temperature difference between the equator and the pole, assuming that ω_r depends only on pressure? The planetary radius is $a = 6100$ km, and the gas constant is $R = 187$ J kg^{-1} K^{-1}.

3.18. Suppose that during the passage of a cyclonic storm the radius of curvature of the isobars is observed to be 800 km at a station where the wind is veering (turning clockwise) at a rate of 10° per hour. What is the radius of curvature of the trajectory for an air parcel that is passing over the station? (The wind speed is 20 m s^{-1}.)

3.19. Show that the divergence of the geostrophic wind in isobaric coordinates on the spherical earth is given by

$$\nabla \cdot \mathbf{V}_g = -\frac{1}{fa}\frac{\partial\Phi}{\partial x}\left(\frac{\cos\phi}{\sin\phi}\right) = -v_g\left(\frac{\cot\phi}{a}\right)$$

(Use the spherical coordinate expression for the divergence operator given in Appendix C.)

3.20. The following wind data were received from 50 km to the east, north, west, and south of a station, respectively: 90°, 10 m s^{-1}; 120°, 4 m s^{-1}; 90°, 8 m s^{-1}; and 60°, 4 m s^{-1}. Calculate the approximate horizontal divergence at the station.

3.21. Suppose that the wind speeds given in Problem 3.20 are each in error by ±10%. What would be the percentage error in the calculated horizontal divergence in the worst case?

3.22. The divergence of the horizontal wind at various pressure levels above a given station is shown in the following table. Compute the vertical velocity at each level assuming an isothermal atmosphere with temperature 260 K and letting $w = 0$ at 1000 hPa.

Pressure (hPa)	$\nabla \cdot \mathbf{V} (\times 10^{-5}\ \mathrm{s}^{-1})$
1000	+0.9
850	+0.6
700	+0.3
500	0.0
300	−0.6
100	−1.0

3.23. Suppose that the lapse rate at the 850-hPa level is 4 K km^{-1}. If the temperature at a given location is decreasing at a rate of 2 K h^{-1}, the wind is westerly at 10 m s^{-1}, and the temperature decreases toward the west at a rate of 5 K/100 km, compute the vertical velocity at the 850-hPa level using the adiabatic method.

MATLAB Exercises

M3.1. For the situations considered in Problems M2.1 and M2.2, make further modifications in the MATLAB scripts to compute the vertical profiles of density and of the static stability parameter S_p defined in (3.7). Plot these in the interval from $z = 0$ to $z = 15$ km. You will need to approximate the vertical derivative in S_p using a finite difference approximation (see Section 13.2.1).

M3.2. The objective of this exercise is to gain an appreciation for the difference between trajectories and streamlines in synoptic-scale flows. An idealized representation of a midlatitude synoptic disturbance in an atmosphere with no zonal mean flow is given by the simple sinusoidal pattern of geopotential,

$$\Phi\,(x, y, t) = \Phi_0 + \Phi' \sin\left[k\,(x - ct)\right] \cos\ ly$$

where $\Phi_0\,(p)$ is the standard atmosphere geopotential dependent only on pressure, Φ' is the magnitude of the geopotential wave disturbance, c is the phase speed of zonal propagation of the wave pattern, and k and l are the wave numbers in the x and y directions, respectively. If it is assumed that the flow is in geostrophic balance, then the geopotential is proportional to the stream function. Let the zonal and meridional wave numbers be equal

($k = l$) and define a perturbation wind amplitude $U' \equiv \Phi' k / f_0$, where f_0 is a constant Coriolis parameter. Trajectories are then given by the paths in (x, y) space obtained by solving the coupled set of ordinary differential equations:

$$\frac{Dx}{Dt} = u = -f_0^{-1}\frac{\partial \Phi}{\partial y} = +U' \sin\left[k\left(x - ct\right)\right] \sin ly$$
$$\frac{Dy}{Dt} = v = +f_0^{-1}\frac{\partial \Phi}{\partial x} = +U' \cos\left[k\left(x - ct\right)\right] \cos ly$$

[Note that U' (taken to be a positive constant) denotes the amplitude of both the x and y components of the disturbance wind.] The MATLAB script **trajectory_1.m** provides an accurate numerical solution to these equations for the special case in which the zonal mean wind vanishes. Three separate trajectories are plotted in the code. Run this script letting $U' = 10\ \mathrm{m\ s^{-1}}$ for cases with $c = 5$, 10, and 15 $\mathrm{m\ s^{-1}}$. Describe the behavior of the three trajectories for each of these cases. Why do the trajectories have their observed dependence on the phase speed c at which the geopotential height pattern propagates?

M3.3. The MATLAB script **trajectory_2.m** generalizes the case of Problem M3.2 by adding a mean zonal flow. In this case the geopotential distribution is specified to be $\Phi(x, y, t) = \Phi_0 - f_0 \bar{U} l^{-1} \sin ly + \Phi' \sin\left[k\left(x - ct\right)\right] \cos ly$.

- **(a)** Solve for the latitudinal dependence of the mean zonal wind for this case.
- **(b)** Run the script with the initial x position specified as $x = -2250$ km and $U' = 15\ \mathrm{m\ s^{-1}}$. Do two runs, letting $\bar{U} = 10\ \mathrm{m\ s^{-1}}$, $c = 5\ \mathrm{m\ s^{-1}}$ and $\bar{U} = 5\ \mathrm{m\ s^{-1}}$, $c = 10\ \mathrm{m\ s^{-1}}$, respectively. Determine the zonal distance that the ridge originally centered at $x = -2250$ km has propagated in each case. Use this information to briefly explain the characteristics (i.e., the shapes and lengths) of the 4-day trajectories for each of these cases.
- **(c)** Which combination of initial position, $\bar{U}$ and c, will produce a straight-line trajectory?

M3.4. The MATLAB script **trajectory_3.m** can be used to examine the dispersion of a cluster of N parcels initially placed in a circle of small radius for a geopotential distribution representing the combination of a zonal mean jet plus a propagating wave with NE to SW tilt of trough and ridge lines. The user must input the mean zonal wind amplitude, $\bar{U}$, the disturbance horizontal wind, U', the propagation speed of the waves, c, and the initial y position of the center of the cluster.

- **(a)** Run the model for three cases specifying $y = 0$, $U' = 15\ \mathrm{m\ s^{-1}}$, and $\bar{U} = 10, 12$, and 15 $\mathrm{m\ s^{-1}}$, respectively. Compute 20-day trajectories for all parcel clusters. Give an explanation for the differences in the dispersion of the parcel cluster for these three cases.
- **(b)** For the situation with $c = 10\ \mathrm{m\ s^{-1}}$, $U' = 15\ \mathrm{m\ s^{-1}}$, and $\bar{U} = 12\ \mathrm{m\ s^{-1}}$, run three additional cases with the initial y specified to be 250, 500, and 750 km.

Describe how the results differ from the case with $y = 0$ km and $\bar{U} = 12\ \mathrm{m\ s^{-1}}$, and give an explanation for the differences in these runs.